# Effect of Laser Irradiation on the Properties of ZnO Buffer Layers and Its Application to Selective-Growth of ZnO Nano/Microcrystals

Tetsuya SHIMOGAKI[*1], Hirotaka KAWAHARA[*1], Shihomi NAKAO[*1], Kosuke HARADA[*1], Mitsuhiro HIGASHIHATA[*1] Hiroshi IKENOUE[*1], Yoshiki NAKARA[*2], Daisuke NAKAMURA[*1], Tatsuo OKADA[*1]

[*1] *Graduate School of Information Science and Electrical Engineering, Kyushu Univ., 744 Motooka, Nishi-ku, Fukuoka 819-0395, Japan*
*E-mail: shimogaki@laserlab.ees.kyushu-u.ac.jp*
[*2] *Faculty of Information Science and Electrical Engineering, Kyushu Univ., 744 Motooka, Nishi-ku, Fukuoka 819-0395, Japan*

ZnO nanocrystals, which are characterized by their configurations and fine structures, are unique oxide semiconductors. They are synthesized by nanoparticle-assisted pulsed laser deposition on ZnO buffer layers deposited on *a*-cut sapphire substrates. In this report, the new possibilities of UV laser-processing to the field of ZnO buffer layers and ZnO nano/microcrystals are suggested. Effects of ultraviolet laser-irradiation on morphological and electrical properties of ZnO buffer layers were investigated. After laser irradiation, surface work function increased in the region laser-irradiated at 300 mJ/cm$^2$, whereas it decreased in the region laser-irradiated at 500 mJ/cm$^2$. Then, ZnO nanowires were synthesized on the ZnO buffer layers locally laser-irradiated at 300 mJ/cm$^2$ and 500 mJ/cm$^2$ by nanoparticle-assisted pulsed laser deposition. Number densities of ZnO nanowires were varied depend on laser fluences. It decreased in the region pre-laser-irradiated at 300 mJ/cm$^2$, whereas it increased in the region pre-laser-irradiated at 500 mJ/cm$^2$. Additionally, it was demonstrated that periodically-aligned ZnO microcrystals can be synthesized using four-beam interference laser irradiation to the ZnO buffer layers followed by nanoparticle-assisted pulsed laser deposition. Since these processes do not require any catalysts, they are expected to be the new fabrication method for ZnO nano/micro crystals.

DOI: 10.2961/jlmn.2015.03.0004
**Keywords:** zinc oxide, nanowire, microcrystal, laser annealing, laser ablation, four-beam interfered laser

## 1. Introduction

Zinc oxide (ZnO), which has abundant natural resources, has a wide band-gap energy of approximately 3.37 eV and a large exciton binding energy of 60 meV. These mean that ZnO can realize an efficient exciton emission in near ultraviolet (UV) spectral region. Accordingly, ZnO is one of the most attracted materials for optoelectronic applications which operate in the UV range. [1, 2] In addition, a variety of ZnO nanocrystals can be synthesized due to self-organization. Besides, a variety of ZnO nanocrystals such as nanowires, nanorods, and nanorings, which are provided by their self-organized growth, have scientific attractiveness because of their unique morphologies. [3, 4, 5] ZnO nanocrystals have quite-small volume and high aspect ratio, so that quantum effect and optical confinement can be expected.

In this paper, we suggest new ideas about the combination of the ZnO crystals and UV laser processing. There are some associated researches. Pulsed-laser deposition (PLD) is a well-known method of fabricating ZnO thin films characterized by a high-throughput. [6, 7] In our early study, nanoparticle-assisted pulsed laser deposition (NAPLD) was established to fabricate ZnO nanocrystals. [8] Additionally, it was found that vertical-growth-degree of ZnO nanowires can be improved using ZnO buffer layer. [9] UV laser annealing on ZnO crystals have been investigated by some researchers. For example, the effect of laser annealing on ZnO thin film was researched and it was found that the surface roughness of ZnO thin films can be decreased. [10] Optical properties of ZnO nanocrystals have been investigated in our previous study. [11]

In this paper, a new idea about the combination of PLD, laser annealing and NAPLD is suggested. Flow chart of experimental procedures were shown in Figure 1. At first, a ZnO buffer layer, which is a kind of ZnO thin films, was laser-annealed at some fluences, then ZnO nanowires were grown on it. The variation in the number density of ZnO nanowires was investigated. Subsequently, periodically-aligned ZnO microcrystals were fabricated using the micro-patterned ZnO buffer layer by irradiating four-beam interfered the third harmonic of Nd:YAG laser.

## 2. Experiment

### 2.1 Preparation of ZnO buffer layers

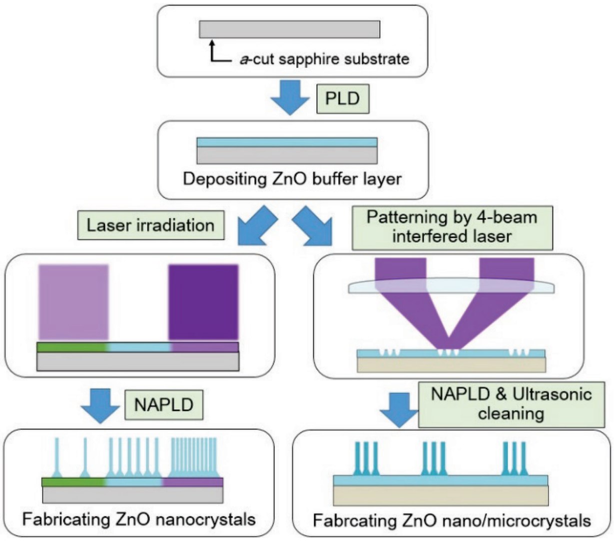


**Fig. 1** Schematic flow chart of experimental procedures.

ZnO thin films, which are called ZnO buffer layers hereafter, were synthesized by PLD. A sintered ZnO target placed in a vacuum chamber was ablated for 5 min with the third harmonic of a Q-switched Nd:YAG laser (λ = 355 nm, pulse width τ = 10 ns, Quanta-ray GCR-290-10, Spectra-Physics) at a fluence of 1.5 J/cm$^2$. The chamber pressure were kept at 3 Pa. ZnO buffer layers were deposited on an *a*-cut sapphire substrate heated at 500 °C, placed at the facing position toward the sintered ZnO target.

## 2.2 Pre-laser annealing and pre-laser ablation

Pre-laser irradiating process was performed with a KrF excimer laser (λ = 248 nm, pulse width τ = 55 ns). The laser beam was scanned over the surface of the ZnO buffer layer using a motorized X-Y stage. The repetition rate and scanning speed were set at 1000 Hz and 3.5 mm/s, which the ZnO buffer layer was irradiated 100 times per location. Laser fluences were 300 mJ/cm$^2$ and 500 mJ/cm$^2$, as shown in Fig. 2(a).

Figure 2(b) and (c) show atomic force microscopy (AFM) and kelvin probe force microscopy (KPFM) images of the boundary between the laser-irradiated region at 300 mJ/cm$^2$ and as-deposited region. Both images were obtained concurrently, so that the observing areas are same. It was found that the root mean square value of the surface RMS roughness (Root-Mean-Square value) of the ZnO buffer layer decreased from 3.136 nm to 0.548 nm by laser irradiating at 300 mJ/cm$^2$. The KPFM image in Fig. 2(c) indicates the increase in the surface work function of ZnO buffer layer by laser irradiation at 300 mJ/cm$^2$, because the mapping parameter of KPFM image, which is the contact potential difference between the cantilever and the surface of the sample ($V_{CPD}$), is represented by the following equation. [12]

$$eV_{CPD} = \Phi_{probe} - \Phi_{sample} \qquad (1)$$

Here, $\Phi_{probe}$ and $\Phi_{sample}$ are the work functions of the cantilever and sample, respectively, and *e* is the elementary charge. Therefore, the contrast of KPFM images provides the information of inversed-contrast of surface work function of the sample.

Figure 2(d) and (e) show the AFM and KPFM images of the boundary between the as-deposited region and laser-irradiated region at 500 mJ/cm$^2$. There are an energy leak and interference of the laser beam, so that as-deposited region have blue area. Additionally, since the region laser-irradiated at a fluence of 500 mJ/cm$^2$ was chipped off due to excess laser fluence, the average surface height decreased by laser irradiation at a fluence of 500 mJ/cm$^2$. The RMS roughness decreased from 3.451 nm to 0.699 nm. Since KPFM contrast is often affected by precipitous variation in surface height, the probe detects the potential with a slight mechanical error at around the boundary in the bottom of half of Fig. 2(e). The KPFM image indicates that the surface work function of ZnO buffer layer was decreased by laser irradiation at a fluence of 500 mJ/cm$^2$.

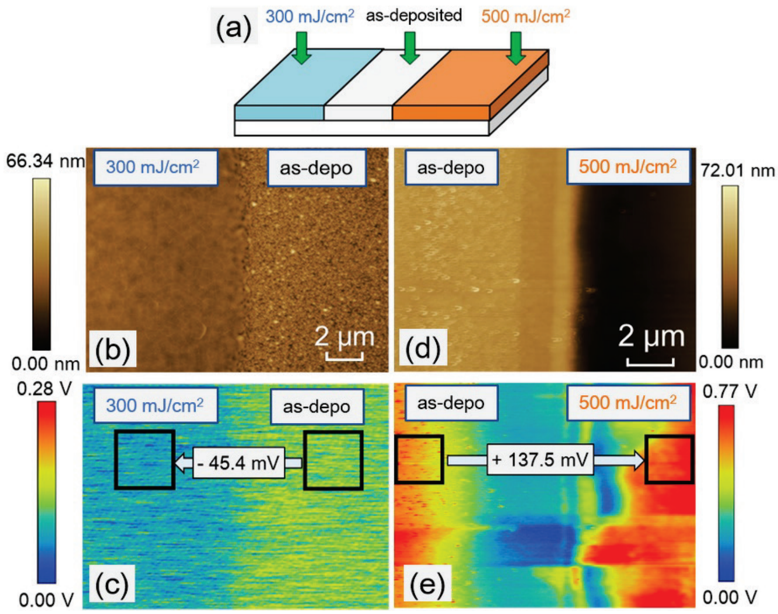


**Fig. 2** (a) Schematic of the laser-irradiated ZnO buffer layer. (b) AFM and (c) KPFM images of the laser-irradiated ZnO buffer layer at the boundary between the laser-irradiated region at 300mJ/cm$^2$ and as-deposited region. (d) AFM and (e) KPFM images of it at the boundary between the as-deposited region and laser-irradiated region at 500 mJ/cm$^2$.

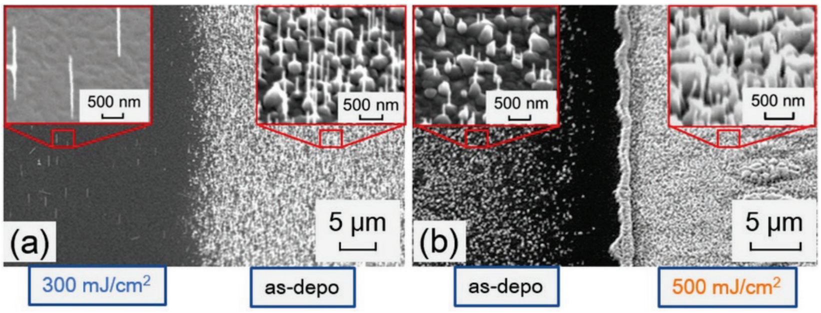


**Fig. 3** Tilted SEM images of ZnO nanowires grown on ZnO buffer layer. (a) At the boundary between pre-laser irradiated region at 300 mJ/cm2 and non-irradiated region and (b) at the boundary between non-irradiated region and pre-laser irradiated region at 500 mJ/cm2.

The variations in properties of ZnO buffer layers can be explained by effects of the laser annealing and laser ablation. Laser irradiation at appropriate fluence can be regarded as a laser annealing process. On the other hand, laser irradiation at excess fluence can be regarded as a laser ablation process. We believe that the decrease in the surface work function of ZnO buffer layers was caused by crystalline defects induced by laser ablation. Additionally, one of the reasons for the increase of work function by laser annealing was the decrease of crystal grain boundaries, where various crystalline defects concentrate. In ZnO crystals, the most susceptible defects are oxygen vacancies and interstitial zincs. [13] Because both defects lead *n*-type conductions, the Fermi level decreased at the laser-annealed region. Accordingly, work functions were increased and decreased at laser-annealed region and laser-ablated region, respectively.

### 2.3 Fabrication of ZnO nanowires on the laser-irradiated ZnO buffer layer

Vertically-aligned ZnO nanowires were fabricated on the pre-laser irradiated ZnO buffer layer, using NAPLD. In this process, ZnO sintered target was ablated for 20 min by the third harmonic of a Q-switched the third harmonic of Nd:YAG laser at the same laser parameters and experimental geometry as PLD. The chamber was filled with Ar gas at a pressure of 26700 Pa. ZnO nanoparticles, which are precursor materials of ZnO nanowires, were generated due to the relatively high pressure. ZnO nanoparticles were deposited on pre-laser irradiated ZnO buffer layer heated at 750 °C.

Figures 3(a) and (b) show the images of ZnO nanowires observed by a scanning electron microscopy (SEM, VE-7800, KEYENCE). The left side of Fig. 3(a) is the pre-laser annealed region at 300 mJ/cm$^2$. It was found that the number density of ZnO nanowires decreased at the pre-laser annealed region at 300 mJ/cm$^2$. On the other hand, it increased at the right side of Fig. 3(b), which is the pre-laser ablated region at 500 mJ/cm$^2$. In both cases, ZnO nanowires were grown on the top of pyramidal crystals, as shown in insets of Fig. 3(a) and (b). The nucleation of pyramidal crystals generally took place at the early stage of NAPLD process.

It was resulted that pre-laser annealing at a moderate fluence decreases the nucleation rates of pyramidal core crystals and ZnO nanowires. On the other hand, pre-laser ablation at an excess fluence increases them. Accordingly,

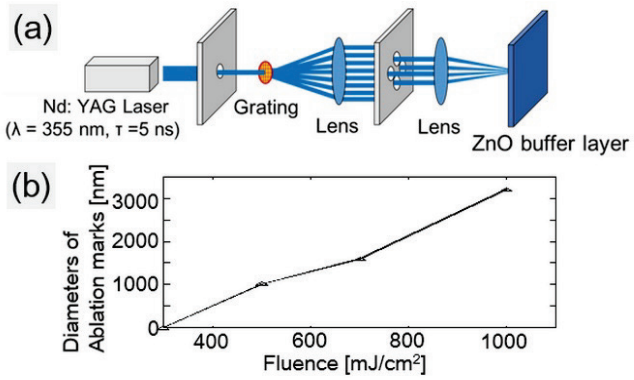


**Fig. 4** (a) Schematic of four-beam laser interference irradiation system. (b) Dependence of diameters of ablation marks on the interference laser fluences.

KPFM images give projections of density of ZnO nanowires in advance of NAPLD process.

### 2.4 Fabrication of ZnO microcrystals by micro patterning with four-beam interfered laser

Next, periodically-aligned ZnO microwires were fabricated by micro-patterning on a ZnO buffer layer with four-beam interference of the third harmonic of a Q-switched Nd:YAG laser (pulse width $\tau$ = 5 ns, Powerlite 8000, Continuum). Micro-patterning and fabrication of meta-material by four-beam interfered laser irradiation were reported by some researchers. [14] We applied it to make micro patterning on ZnO buffer layers followed by NAPLD. Figure 4(a) shows a schematic diagram of four-beam interference laser irradiation system. The incident laser was diffracted by the transmission grating, then diffracted lasers are collimated by a lens. Four first-order diffracted beams were extracted using a slit, then they were focused by another lens. Figure 4(b), where dependence of diameters of ablation marks on the interference laser fluences, indicates that the size of patterns can be controlled.

Figure 5(a) shows a SEM image of the micro-patterned ZnO buffer layer. It was found that ablation marks with diameters of less than 2.0 µm were periodically-aligned on the ZnO buffer layer. They were fabricated on the area of $2.0\times10^4$ µm$^2$ by only the one pulse irradiation at a fluence of 700 mJ/cm$^2$. AFM and KPFM images, which are shown in Figs. 5(b) and (c), indicate that the laser-ablated region had lower surface work functions. According to the results as mentioned in section 2.2 and 2.3, densely-packed ZnO nanowires can be grown on laser-ablated region.

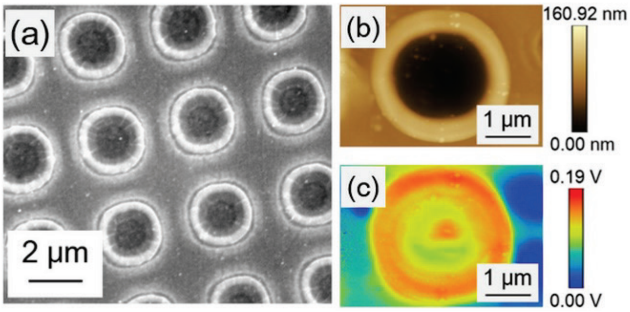


**Fig. 5** (a) The SEM image of periodically micro-patterned ZnO buffer layer. (b) The AFM image of the ablated mark. (c) The KPFM image of the ablated mark.

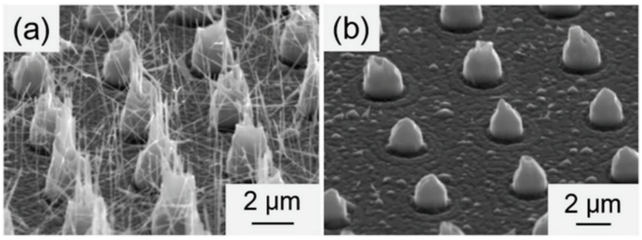


**Fig. 6** (a) The SEM image of ZnO microcrystals and nanowires grown on the periodically micro-patterned ZnO buffer layer and (b) its SEM image after ultrasonic cleaning process.

ZnO microcrystals and nanowires were grown on the micro-patterned ZnO buffer layer by NAPLD. Same experimental conditions were employed as those of section 2.3. Figure 6(a) shows a 40° tilted-view SEM image of as-grown ZnO nano/microcrystals. The surface of ZnO microcrystals were covered with many randomly-grown ZnO nanowires. These nanowires were removed by ultrasonic cleaning process, so that periodically-aligned ZnO microcrystals were remained, as shown in Fig. 6(b).

When the diameter of patterns is larger, ZnO microcrystals have hollow structures. [9] Therefore, we believe that ZnO microcrystals were formed by coalescing ZnO nanowires each other. These ZnO microcrystals with diameters of 1.5 μm can be applied to fabricate field emitter arrays and ZnO microcrystals-based LED arrays without catalyst. Furthermore, the diameter and aspect ratio of periodically-aligned ZnO microcrystals can be controlled by adjusting laser parameters such as the fluence and pulse width as indicated in Fig. 4(b).

## 3. Conclusion

We found that the number density of ZnO nanowires is affected by pre-laser irradiation on ZnO buffer layers. Decreasing effect of ZnO nanowires was observed at pre-laser annealed ZnO buffer layer at 300 $mJ/cm^2$. Increasing effect of ZnO nanowires was determined at pre-laser ablated ZnO buffer layer at 500 $mJ/cm^2$. It was found that work functions were varied depending on laser fluences by the investigation about surface modification on ZnO buffer layer of laser irradiation by KPFM. Additionally, it was found that more densely-packed ZnO nanowires can be grown on the region with lower work function by NAPLD. KPFM can be a new intuitive method to evaluate locational surface properties of ZnO thin films. Finally, periodically-aligned ZnO microcrystals were fabricated on micro-patterned ZnO buffer layer using four-beam interfered laser. Since these techniques require only UV laser processing, they can develop the application of ZnO micro/nano crystals due to their high-throughput.

## Acknowledgments

This work was supported by a Grant-in-Aid for Scientific Research from the Japan Society for the Promotion of Science (JSPS, No. 25286071).

## References

[1] J. H. Lim, C. K. Kang, K. K. Kim, I. K. Park, D. K. Hwang, and S. J. Park: Adv. Mater., 18, (2006) 2720.
[2] S. Chu, J. H. Lim, L. J. Mandalapu, Z. Yang, L. Li, and J. L. Liu: Appl. Phys. Lett., 92, (2008) 152103.
[3] H. Zhang, J. Feng, J. Wang, and M. Zhang: Materials Letters, 61, (2007) 5202.
[4] Y. W. Heo, V. Varadarajan, M. Kaufman, K. Kim, and D. P. Norton: Appl. Phys. Lett., 81, 3046 (2002) 3048.
[5] Z. L. Wang: Materialstoday, 7, (2004) 26.
[6] T. Ohshima, R. K. Thareja, T. Ikegami, and K. Ebihara: Surface and Coating Technology, 169-170, (2003) 517.
[7] V. Craciun, J. Elders, J. G. E. Fardeniers, and I. W. Boyd: Appl. Phys. Lett., 65, (1994) 2963.
[8] R. Q. Guo, J. Nishimura, M. Matsumoto, D. Nakamura, and T. Okada: Appl. Phys. A, 93, (2008) 843.
[9] D. Nakamura, T. Shimogaki, S. Nakao, K. Harada, Y. Muraoka, H. Ikenoue, and T. Okada: J. Phys. D: Appl. Phys., 47, (2014) 034014.
[10] Y. Zhao, and Y. Jiang: J. Appl. Phys., 103, (2008) 114903.
[11] T. Shimogaki, K. Okazaki, D. Nakamura, M. Higashihata, T. Asano, and T. Okada: Opt. Express, 20, (2012) 15247.
[12] S. Kurbanov, W. C. Yang, and T. W. Kang: Appl. Phys. Express, 4, (2011) 021101.
[13] K. H. Tam, C. K. Cheung, Y. H. Leung, A. B. Djurišić, C. C. Ling, C. D. Beling, S. Fung, W. M. Kwok, W. K. Chan, D. L. Phillips, L Ding, and W. K. Ge: J. Phys. Chem. B, 110, (2006) 20865.
[14] Y. Nakata, N. Miyanaga, and T. Okada: Applied surface Science, 253, (2007) 6555.

(Received: June 27, 2014, Accepted: May 20, 2015)